nature nanotechnology

SUPPLEMENTARY INFORMATION

DOI: 10.1038/NNANO.2013.227

High-throughput optical imaging and spectroscopy of individual carbon nanotubes in devices

Kaihui Liu*[1], Xiaoping Hong*[1], Qin Zhou[1], Chenhao Jin[1], Jinghua Li[2], Weiwei Zhou[2], Jie Liu[2], Enge Wang[3], Alex Zettl[1,4], Feng Wang[1,4]

DOI: 10.1038/NNANO.2013.227

S1. Mechanism of optical contrast of nanotubes on fused silica in our polarization-based microscopy.

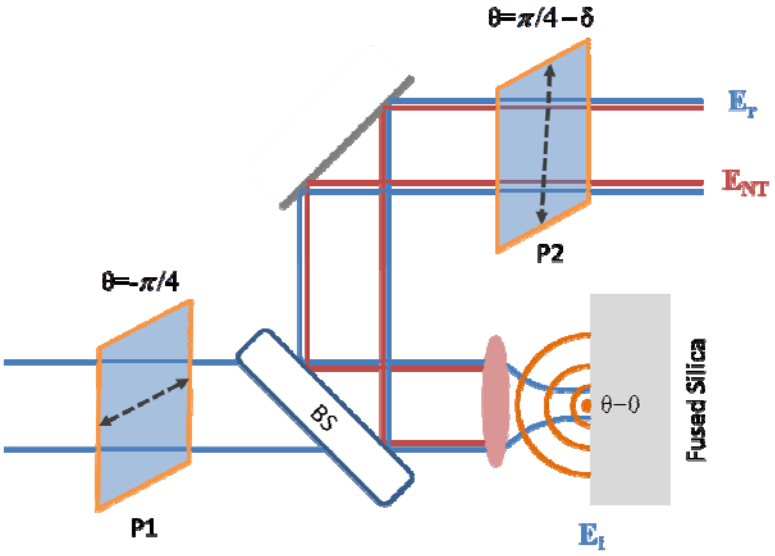

Figure S1. Scheme of electric field propagation in our reflection microscope with two polarizers

Optical contrast of carbon nanotube on substrates is directly related to the optical susceptibility of the nanotube. Here we examine quantitatively the contrast mechanism using nanotubes on a fused silica substrate as an example.

The nanotube contrast at the imaging camera is determined by interference of the electrical field from nanotube and the reflected field, and it can be described by

$$\frac{\Delta I}{I} = \frac{\left|E_{NT} + E_r\right|^2 - \left|E_r\right|^2}{\left|E_r\right|^2} = \frac{2\,\mathrm{Re}(E_r E_{NT}^{\ *})}{\left|E_r\right|^2} \qquad \text{(S1)}$$

In the far field, $E_r = (rE_i e^{-i\pi/2})\sin\delta$ and $E_{NT} = (1+r)^2 \chi E_i / 2$, where E_i is the incident electric field at the sample, r=-0.2 is the Fresnel reflection factor for fused silica, δ is the deviation angle from the crossed polarization, and χ is the optical susceptibility of carbon nanotube. The term $e^{-i\pi/2}$ describes the Gouy phase associated with the reflection light that has propagated through

the focus to far field. The $(1+r)^2$ term describes the local electrical field at the substrate experienced by the nanotube relative to the E_{in}. Using these parameters we obtain the optical contrast of a nanotube $\frac{\Delta I}{I} = -3.2\frac{\mathrm{Im}(\chi)}{\sin\delta}$.

In this case, the optical contrast is exactly proportional to the Im(χ) of the nanotube. The sign of optical contrast depends on the angle δ. Therefore the nanotube can appear brighter or darker than the environment depending on the sign of the second polarizer deviation from vertical direction.

The situation for nanotube on other substrates can be similarly analyzed. For Si wafer with 90 nm SiO_2, the nanotube optical spectra is dominated by Im(χ) over the whole visible spectral range. With an arbitrary substrate, the nanotube contrast in general will depend on the complex susceptibility because Fresnel reflection factor is usually complex. In such cases, the resonance energy of optical transitions can still be obtained reliably, although the resonance lineshape can be distorted.

S2: Gating efficiency calibration using G-mode Raman resonance in metallic nanotubes

We calibrated the gating efficiency of our field-effect device by characterizing the gate-dependent G-mode Raman peak in non-armchair metallic carbon nanotubes[1]. Figure S2 shows one calibration example from a (13,1) nanotube on 90nm SiO_2/Si substrate with back-gate field-effect transistor geometry. Doping in metallic nanotube blocks the low energy electronic transitions, and it changes the coupling between electrons and the longitudinal optical (LO) phonon. A quantitative fitting of this effect on G-mode Raman peak shift and linewidth change for (13,1) nanotube are presented in Fig. S2b and S2c, respectively. From the theoretical fitting,

DOI: 10.1038/NNANO.2013.227

we can deduce a gating efficiency of 0.013 hole/(nm.V) for line charge density in this (13,1) nanotube (diameter = 1.1 nm).

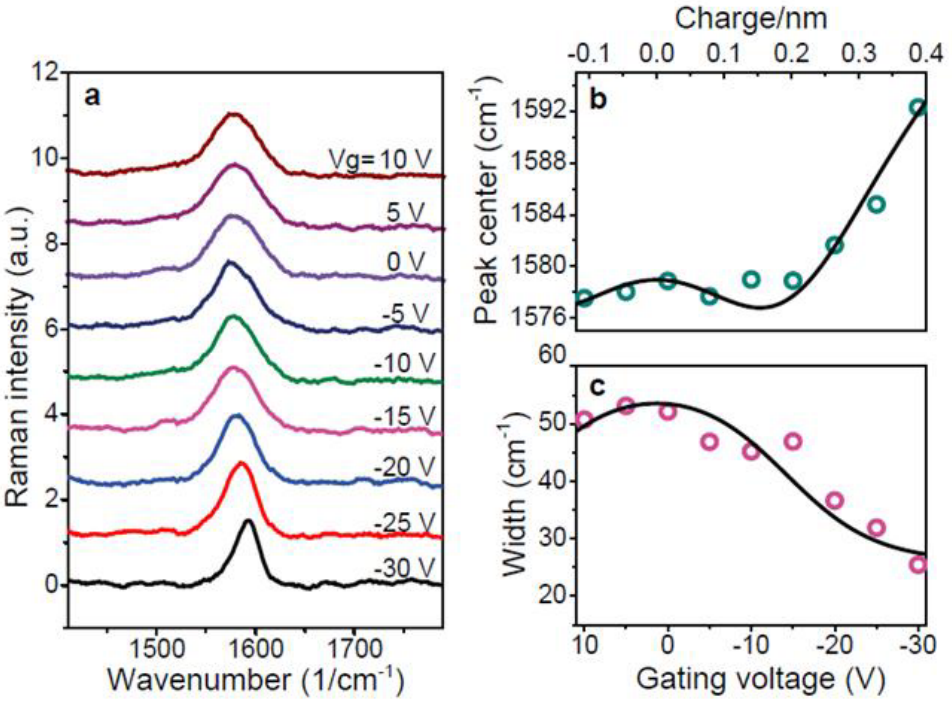

Figure S2. (**a**) G-mode Raman spectra for (13, 1) metallic nanotube at different back-gated voltages. (**b**)(**c**) Changes in the Raman peak center (b) and width (c) as a function of gating voltages (dots). Solid lines are based on fitting using the model in Ref. 1, which relate the G-mode Raman to carrier concentration in the metallic nanotube (top axis). Comparison between the experiment and theory yields the gating efficiency of this nanotube field-effect transistor.

For nanotubes of different diameter, the classic capacitance scales with $1/\ln(4t/d)$, where t is thickness of dielectric layer and d is the nanotube diameter. Therefore this gating efficiency varies with the diameter only weakly in a logarithmic dependence. (At the relatively high gating voltages used here, quantum capacitance of the nanotube is not important[2]). We calibrated three metallic nanotubes and found that the gating efficiencies are similar in these devices, with a variation less than 30% after accounting for the diameter dependent capacitance.

S3. Estimation for dielectric screening effect on the optical transition linewidth

It has been shown previously that dielectric environment can induce significant redshift in the exciton transition energy, but has relative weak effects on the broadening of the resonance peak. For example, optical resonances of SWNTs in micelle solution are typically redshifted by 20 meV from those of suspended SWNTs, but the width change is less than 10 meV (ref 3, 4). In another example, the optical resonances are shifted by 30~50 meV due to screening from other tubes in bundles but linewidth broadening is negligible[5]. In our experiment, the energy redshift is ~ 30 meV. It indicates resonance width broadening from the dielectric screening is less than 15 meV. Experimentally we observed a gate-induced broadening of more than 50 meV. This large broadening beyond the dielectric screening effect can be accounted for by the Auger process that we described in the text.

S4. Optical spectra of SWNT (16,8) at significantly different positions

For our single-wall nanotube on substrate, the optical spectrum remains the almost identical along the entire nanotube. Figure S3 shows several optical spectra measured along the same (16,8) nanotube of up to 1 mm long. The optical spectra are almost identical, similar to that observed in suspended SWNTs[6]. This behaviour suggests that the observed resonance linewidth is largely due to homogeneous broadening in the nanotube.

DOI: 10.1038/NNANO.2013.227

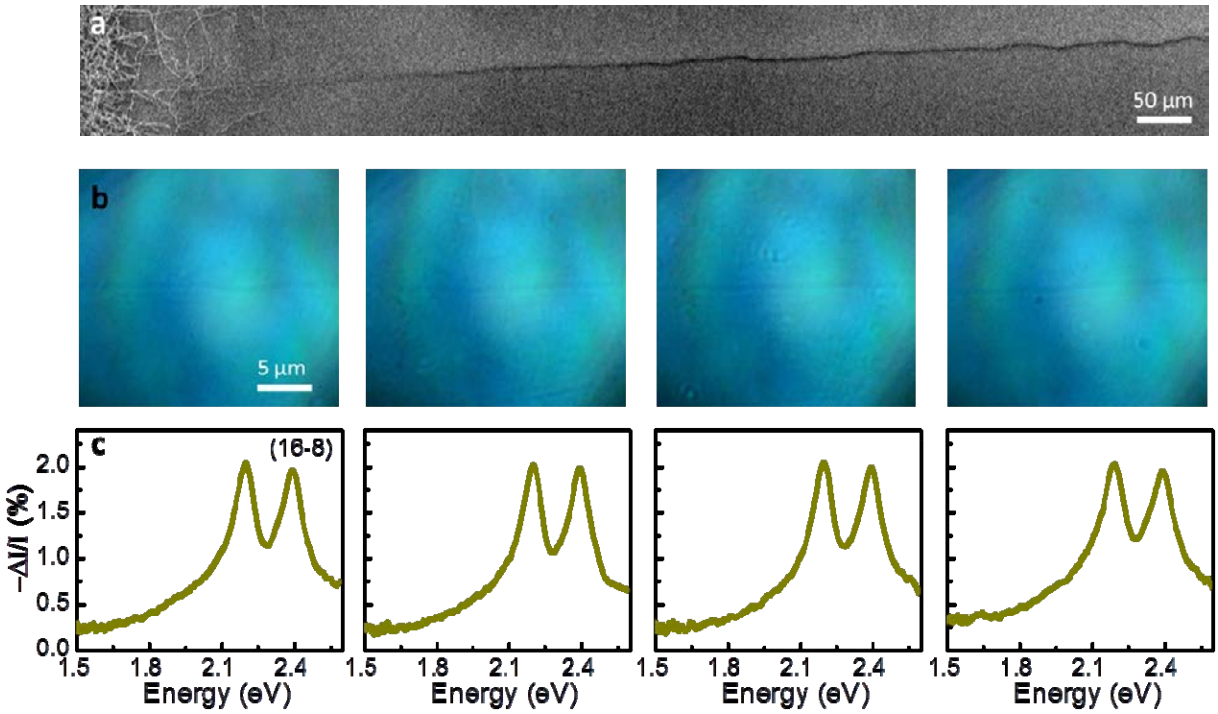

Figure S3. (a) SEM image of the SWNT (16,8). (b) Optical image of the same nanotube at different postions with distance ~250 um away. (c) Optical spectra of the nanotube corresponded to the center positions of (b).

S5: Schematics for all four different inter-subband scattering channels between free holes and optical excited electrons in a doped metallic nanotube that can contribute to the ultrafast dephasing of the exciton.

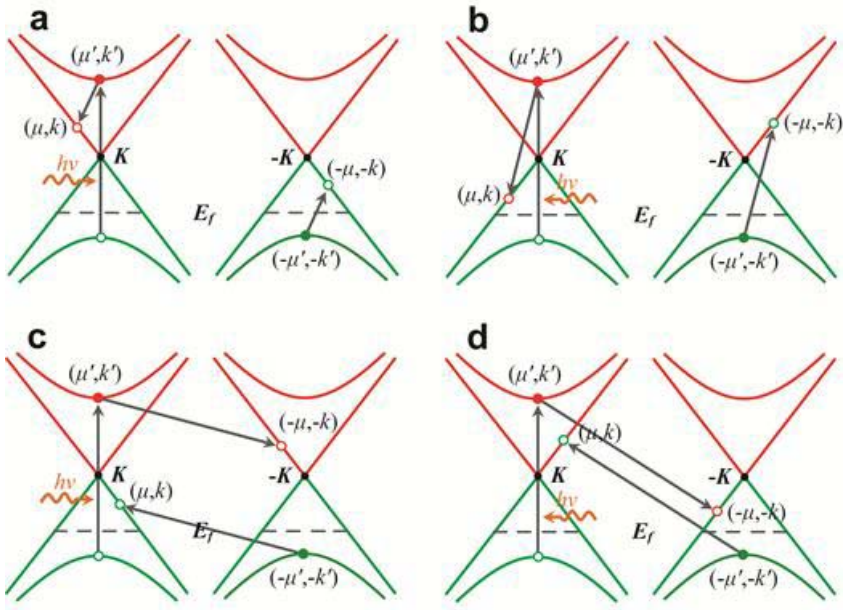

Figure S4. Four representative electron scattering channels that satisfy the energy, momentum and angular momentum conservation requirement in doped metallic nanotubes

The picture is quite similar for semiconducting nanotubes, except that the lowest band is parabolic instead of linear as in metallic nanotube.

S6. Supplementary Movie caption

Real-time video of tracing a carbon nanotube sample on SiO_2/Si substrate using our polarization-based homodyne microscopy. The view size is ~30 microns in diameter.

- 00:01: Upper-right part of the nanotubes is under Al_2O_3 layer; Lower-left part of the nanotubes is on SiO_2/Si substrate.
- 00:39: A few different nanotubes appear.
- 02:10: Another nanotube perpendicular to the first one is seen with opposite contrast, as predicted by the polarization-based homodyne method when the nanotube orientation changes from 45 to 135 degrees.

DOI: 10.1038/NNANO.2013.227

- 02:27 Upper-right part of the nanotubes is on SiO_2/Si substrate; Lower-left part of the nanotubes is under Al_2O_3 layer.

References:

1 Tsang, J. C. *et al.* Doping and phonon renormalization in carbon nanotubes. *Nature Nanotechnology* 2, 725-730 (2007).

2 Ilani, S., Donev, L. A. K., Kindermann, M. & McEuen, P. L. Measurement of the quantum capacitance of interacting electrons in carbon nanotubes. *Nature Physics* 2, 687-691 (2006).

3 Bachilo, S. M. *et al.* Structure-assigned optical spectra of single-walled carbon nanotubes. *Science* 298, 2361-2366 (2002).

4 Lefebvre, J., Fraser, J. M., Homma, Y. & Finnie, P. Photoluminescence from single-walled carbon nanotubes: a comparison between suspended and micelle-encapsulated nanotubes. *Appl Phy a* 78, 1107-1110 (2004).

5 Wang, F. *et al.* Interactions between individual carbon nanotubes studied by Rayleigh scattering spectroscopy. *Phys Rev Lett* 96, 167401 (2006).

6 Sfeir, M. Y. *et al.* Probing electronic transitions in individual carbon nanotubes by Rayleigh scattering. *Science* 306, 1540-1543 (2004).